Thermal, Chemical, and Enzymatic Stability of the Cyclotide Kalata B1: The Importance of the Cyclic Cystine Knot†

Michelle L. Colgrave and David J. Craik*

Institute for Molecular Bioscience, University of Queensland, Brisbane 4072, Australia

Received February 8, 2004; Revised Manuscript Received March 18, 2004

ABSTRACT: The cyclotides constitute a recently discovered family of plant-derived peptides that have the unusual features of a head-to-tail cyclized backbone and a cystine knot core. These features are thought to contribute to their exceptional stability, as qualitatively observed during experiments aimed at sequencing and characterizing early members of the family. However, to date there has been no quantitative study of the thermal, chemical, or enzymatic stability of the cyclotides. In this study, we demonstrate the stability of the prototypic cyclotide kalata B1 to the chaotropic agents 6 M guanidine hydrochloride (GdHCl) and 8 M urea, to temperatures approaching boiling, to acid, and following incubation with a range of proteases, conditions under which most proteins readily unfold. NMR spectroscopy was used to demonstrate the thermal stability, while fluorescence and circular dichroism were used to monitor the chemical stability. Several variants of kalata B1 were also examined, including kalata B2, which has five amino acid substitutions from B1, two acyclic permutants in which the backbone was broken but the cystine knot was retained, and a two-disulfide bond mutant. Together, these allowed determinations of the relative roles of the cystine knot and the circular backbone on the stability of the cyclotides. Addition of a denaturant to kalata B1 or an acyclic permutant did not cause unfolding, but the two-disulfide derivative was less stable, despite having a similar three-dimensional structure. It appears that the cystine knot is more important than the circular backbone in the chemical stability of the cyclotides. Furthermore, the cystine knot of the cyclotides is more stable than those in similar-sized molecules, judging by a comparison with the conotoxin PVIIA. There was no evidence for enzymatic digestion of native kalata B1 as monitored by LC−MS, but the reduced form was susceptible to proteolysis by trypsin, endoproteinase Glu-C, and thermolysin. Fluorescence spectra of kalata B1 in the presence of dithiothreitol, a reducing agent, showed a marked increase in intensity thought to be due to removal of the quenching effect on the Trp residue by the neighboring Cys5−Cys17 disulfide bond. In general, the reduced peptides were significantly more susceptible to chemical or enzymatic breakdown than the oxidized species.

The cyclotides constitute a family of macrocyclic peptides with unique structural and biophysical properties (*1*). Although its structure was not known at the time, the prototypic member of the family was first discovered in the 1970s by Red Cross workers in Africa. They noted that during childbirth women of the Lulua tribe made use of the medicinal properties of a native plant *Oldenlandia affinis*, or "kalata kalata" as it is locally known (*2*, *3*). A tea made from the leaves of the plant was used to accelerate uterine contractions and childbirth. The preparation by boiling and the oral administration suggested that the active ingredient was both thermally stable and bioavailable. Subsequent investigations revealed that the peptide kalata B1 was responsible for the uterotonic activity (*4*). In early studies aimed at characterizing it, kalata B1 was shown to be resistant to proteolytic degradation and retained its activity after heating (*5*). The peptide was subsequently shown to comprise 29 amino acids, including six cysteine residues (*6*). The structure determined using NMR revealed the unique features of a head-to-tail cyclized backbone and a core composed of three disulfide bonds arranged in a cystine knot motif. In this motif, an embedded ring in the structure, formed by two disulfide bonds and their connecting backbone segments, is penetrated by the third disulfide bond. The combination of a cystine knot motif embedded within a circular backbone is termed a cyclic cystine knot (CCK)[1] (*1*, *7*).

Over the past decade, numerous examples of peptides containing a macrocyclic backbone and conserved Cys residues that are characteristic of a CCK motif have been reported (*1*, *2*, *6*, *8*−*23*) and are collectively known as the cyclotides. The cyclotides exhibit a diverse range of biological activities, including insecticidal (*22*), anti-HIV (*9*),

† This work was supported in part by a grant from the Australian Research Council (D.J.C.). D.J.C. is an Australian Research Council Senior Fellow.

* To whom correspondence should be addressed: Institute for Molecular Bioscience, University of Queensland, Brisbane, Australia. Phone: +61 7 3346 2019. Fax: +61 7 3346 2029. E-mail: d.craik@imb.uq.edu.au.

[1] Abbreviations: CCK, cyclic cystine knot; GdHCl, guanidine hydrochloride; DTT, dithiothreitol; ESI, electrospray; LC−MS, liquid chromatography mass spectrometry; CD, circular dichroism; kB1, kalata B1; kB2, kalata B2; kB1-RA, reduced, alkylated kalata B1; DnaK-f, truncated form of *Escherichia coli* DnaK 577−610; endoGlu-C, endoproteinase Glu-C.

10.1021/bi049711q CCC: $27.50
Published on Web 05/01/2004

antimicrobial (*14*), anti-neurotensin (*10*), cytotoxic (*24*), and hemolytic (*25*) properties. The toxic functions of the cyclotides have led to suggestions that they are present in plants for defense purposes (*1*). They constitute one of a number of families of head-to-tail cyclic proteins that have been discovered over the past few years in bacteria, plants, and animals (*26*).

The cystine knot structural motif has been found in many peptides and proteins, including examples from plants, fungi, marine molluscs, insects, and spiders (*7*). The motif was formally named in 1993 when the structural similarities between a number of growth factors were reported (*27*, *28*). Earlier studies had identified a "knottin" fold in squash family plant proteins (*29*). Cystine knots can be classified into three types: the inhibitor cystine knots, where the $Cys^{III}-Cys^{VI}$ bond penetrates the ring formed by the $Cys^{I}-Cys^{II}$ and $Cys^{IV}-Cys^{V}$ bonds (*30*), the growth factor cystine knots, where the $Cys^{I}-Cys^{IV}$ bond penetrates the ring formed by the $Cys^{II}-Cys^{III}$ and $Cys^{V}-Cys^{VI}$ bonds (*31*), and the cyclic cystine knot mentioned above (*7*). Studies of molecules from the first two classes have demonstrated the crucial importance of the knot in defining structure and biological activity. For example, the disulfide connectivity for the AVR9 elicitor of a fungal tomato pathogen (*32*) is identical to that of the cyclotide family: $Cys^{I}-Cys^{IV}$, $Cys^{II}-Cys^{V}$, and $Cys^{III}-Cys^{VI}$. The necrosis-inducing activity of this fungal avirulence protein was completely lost upon removal of any of the three disulfide bonds (*33*). A number of the conotoxins, including the μ-, δ-, and ω-conotoxins, and at least one member of the κ-conotoxins contain the cystine knot motif (*34*). Studies on the ω-conotoxin MVIIA indicated that removing any of the disulfide bonds greatly destabilized the native structure (*35*). Vascular endothelial growth factor (VEGF) belongs to the growth factor cystine knot protein family. Removal of individual disulfide bonds via mutations of this protein did not reduce its thermodynamic stability, but did reduce its thermal stability and caused a ~40 °C decrease in its melting temperature (*36*). Furthermore, proteolysis studies showed that misfolded forms resulting from cystine deletion mutants of the VEGF protein were degraded rapidly relative to native VEGF (*37*).

So far, there have been no systematic studies on the role of the cystine knot in defining the stability of the cyclotides. The cyclic backbone of the cyclotides also potentially confers advantages over conventional linear proteins, including greater stability and resistance to proteolytic digestion; since circular proteins have no termini, they are resistant to cleavage by exopeptidases. It has been suggested that the rigid nature and stability of the cyclotide framework make it useful as a scaffold in drug design (*7*, *38*). Therefore, it was of interest to quantitatively determine the thermal, chemical, and enzymatic stability of this class of molecules and to examine the roles of the disulfide bonds and the cyclic backbone in stabilizing the structure. This has been done by monitoring a range of biophysical markers of the prototypic cyclotide kalata B1 and several variants under a range of solution conditions.

Figure 1 shows the generic CCK framework and the amino acid sequence of kalata B1 and the variants examined in this study. Kalata B2 is a naturally occurring variant that differs from kalata B1 in five residues. Kalata B1 and kalata B2 both have exposed hydrophobic patches (*39*), and slight

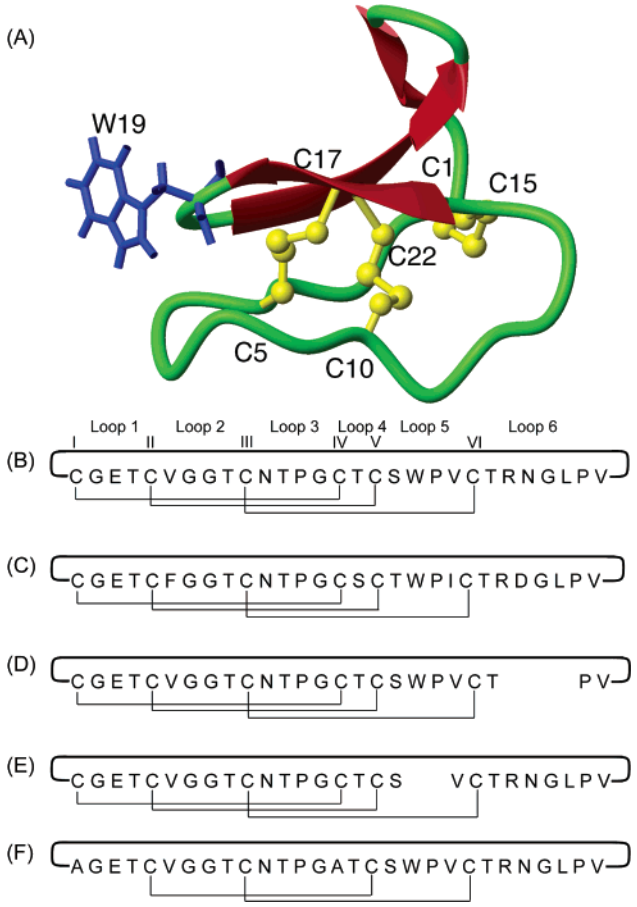

FIGURE 1: Three-dimensional structure (A) and amino acid sequence (B) of kB1. The six conserved Cys residues are numbered with Roman numerals, and the backbone loops between successive Cys residues are numbered 1−6. The structure of kB1 shows the cyclic cystine knot motif and the three disulfide bonds that occupy the core of the molecule. The side chain of the solvent-exposed tryptophan present in loop 5 is shown. The amino acid sequences of kB2, des(24−28)kB1, des(19−20)kB1, and $[A^{1,15}]$kB1 with their associated disulfide bridges are given in parts C−F, respectively. The cysteines are labeled I−VI, and the loops are labeled loop 1−loop 6.

differences in these surface patches are responsible for the self-aggregation of kalata B2 into tetramers and octamers; kalata B1 remains in a monomeric form up to millimolar concentrations. The acyclic permutant, des(24−28)kalata B1, and the disulfide-deficient mutant, $[A^{1,15}]$kalata B1, were investigated to examine the role of the backbone and the contribution of the disulfide core to the overall stability. The former mutant involves the removal of residues 24−28 from the peptide backbone, which is no longer cyclic and thus mimics the conventional cystine knot topology. The latter mutant effectively removes one of the three native disulfide bonds, but adopts a three-dimensional structure similar to that of the native peptide (*40*). Figure 1 also highlights the location of an exposed Trp residue in kalata B1 that is present in all but one of the variants. Normally hydrophobic residues such as Trp would be buried in the interior of the protein, but the tight cystine knot core leaves no room for this and other hydrophobic residues. This Trp provides a probe for fluorescence studies, which were used in combination with a variety of other biophysical measurements in the current study to examine the stability of the CCK motif.

MATERIALS AND METHODS

Isolation. Native kalata B1 (kB1) was isolated from the above-ground parts of *Oldenlandia affinis*. Fresh plant material (500 g) was ground and extracted with a 50/50 (v/v) DCM/MeOH mixture, and the crude extract was partially purified by RP flash chromatography, yielding a fraction containing predominantly cyclotides (5 g). This sample was purified further by preparative RP-HPLC to yield pure kalata B1 (125 mg) as described previously (*1*).

Synthesis of Mutants. Three permutants were synthesized using solid phase methods as described previously (*40*, *41*). Briefly, the peptides were assembled using manual solid phase peptide synthesis with Boc chemistry. Amino acids were added to the resin using HBTU with *in situ* neutralization. Cleavage of the peptides from the resin was achieved using hydrogen fluoride with *p*-cresol and *p*-thiocresol as scavengers [9/0.5/0.5 (v/v) HF/cresol/thiocresol mixture]. The crude reduced peptides were purified on a Phenomenex C_{18} column. Gradients of 0.05% aqueous TFA and 90% acetonitrile with 0.045% TFA were employed with a flow rate of 8 mL/min, and the eluent was monitored at 230 nm. These conditions were used in subsequent purification steps. Cyclization of the [$A^{1,15}$]kB1 mutant was performed in 0.1 M sodium phosphate (pH 7.4) with an excess of TCEP over a period of approximately 30 min. Oxidation of reduced peptides was achieved by dissolving them in a 50/50 (v/v) 0.1 M ammonium bicarbonate (pH 8.5)/2-propanol (0.5 mg/mL) mixture with reduced glutathione added (final concentration of 1 mM). The mixture was stirred at room temperature for 24 h and then purified by RP-HPLC. Correctly folded des(24−28)kB1, des(19−20)kB1, and [$A^{1,15}$]kB1 were identified by their late elution under reverse phase conditions, and ^{1}H NMR spectra confirmed the folded states.

Reduction and Alkylation. kB1 (M_r = 2892 Da) was reduced in ∼4 mM dithiothreitol (DTT) at 37 °C for 1 h in the dark in the presence of 6 M guanidine hydrochloride (GdHCl). An excess of iodoacetamide was then added to alkylate the free sulfur groups present on the six cysteines. The resulting alkylated peptide was then purified by HPLC, lyophilized, and stored at −20 °C until it was used. The peptide was analyzed by mass spectrometry to ensure that alkylation was complete (M_r = 3240 Da). Electrospray mass spectra (not shown) were acquired on solutions of 50 μM kB1 in the presence and absence of 5 mM DTT to confirm that complete reduction had occurred and to look for the presence of any oligomeric species. Peaks were observed at *m*/*z* 1446.8 and 964.9, representing the $[M + 2H]^{2+}$ and $[M + 3H]^{3+}$ ions, respectively, of native kalata B1 (M_r = 2892 Da). Peaks were observed at *m*/*z* 1449.8 and 966.9, representing the $[M + 2H]^{2+}$ and $[M + 3H]^{3+}$ ions, respectively, of reduced kalata B1 (M_r = 2898 Da).

Sample Preparation. Peptide solutions were prepared by dissolving 1 mg of purified peptide in 1 mL of MilliQ H_2O and determining the concentration from the absorbance at 280 nm. Stock solutions of ∼8 M GdHCl were prepared in phosphate buffer (pH 7.4), and their concentrations were determined by refractive index measurement. Urea stock solutions were prepared at concentrations of ∼10 M and quantitated by both gravimetric and refractive index measurements. The final concentration of urea in working solutions was 8 M. A stock solution of 100 mM DTT was prepared in MilliQ H_2O.

NMR Spectroscopy. One-dimensional (1D) ^{1}H NMR spectra were acquired on a Bruker ARX-500 NMR spectrometer at temperatures in the range of 290−370 K. Spectra were processed on a Silicon Graphics Indigo workstation using XWINNMR (Bruker) software.

Fluorescence Spectroscopy. Fluorescence emission spectra were measured between 280 and 500 nm on a Perkin-Elmer luminescence spectrometer using an excitation wavelength of 280 nm and quartz cuvettes with an optical path length of 4 mm. The excitation and emission slit widths were set to 4 nm with a photomultiplier voltage of 650 V. Experiments were performed at 25 °C with the temperature maintained using a Grant LTD6 temperature control unit. All peptide emission spectra were corrected by background subtraction of the spectrum from the equivalent buffer at the given GdHCl concentration and were the average of three scans. Using mellitin as a positive control and kB1 as a test compound, the optimum sample concentration for fluorescence measurement was determined. Solutions containing 25 μM peptide and DTT were prepared and incubated at 37 °C for 30 min; GdHCl was then added and the mixture incubated at room temperature prior to analysis. The final concentration of DTT in the solutions was 5 mM, and the GdHCl concentration ranged between 0 and 6 M.

CD Spectroscopy. CD measurements were carried out on a Jasco J-710 spectropolarimeter with a Neslab RTE-111 temperature control unit. Ellipticity changes at 220 nm were monitored to follow the unfolding transitions in the far-UV region (190−250 nm). All experiments were conducted in the range of 5−90 °C. A path length of 1 mm was used, and all spectra were the average of three scans at a scan speed of 20 nm/min. Solutions of kB1 (50 μM) were prepared in 10 mM potassium phosphate (pH 2.5) in the presence and absence of 8 M urea as described previously (*42*).

Enzymatic Digests. Peptide solutions were dissolved in appropriate buffers at a concentration of 1 mg/mL. Trypsin, endoprotease Glu-C (endoGlu-C), pepsin, and thermolysin (Sigma-Aldrich) were prepared as 1 mg/mL stock solutions in MilliQ H_2O. These were then diluted in appropriate buffers to give a final working solution with a concentration of 20 μg/mL. Trypsin and endoGlu-C were prepared in 100 mM ammonium bicarbonate (pH 8.1). Pepsin digestions were undertaken in a 100 mM acetic/formic acid solution (pH 2.1). Thermolysin was prepared in 100 mM ammonium bicarbonate (pH 8.1) containing 10 mM $CaCl_2$ as an enzymatic cofactor. Digestions using trypsin, endoGlu-C, and pepsin were conducted at 37 °C, while thermolysin was incubated at 65 °C. Equal volumes of peptide and enzyme working solutions were mixed to yield a final substrate/enzyme ratio of 50/1 in all cases. Aliquots (1 μL) were taken at appropriate time intervals and diluted 100-fold in H_2O for immediate analysis by LC−MS or acidified and run at a later time.

Acid Hydrolysis. Solutions containing 1 mg/mL kB1 in either 0.5, 1, or 2 M HCl were incubated at 80 and/or 25 °C to examine the stability of each peptide in acid. At specified times, 1 μL aliquots were removed and diluted 100-fold in water containing sufficient NaOH to neutralize the acid and hence stop the hydrolysis. The resulting solutions were analyzed using LC−MS as described below. DnaK-f and

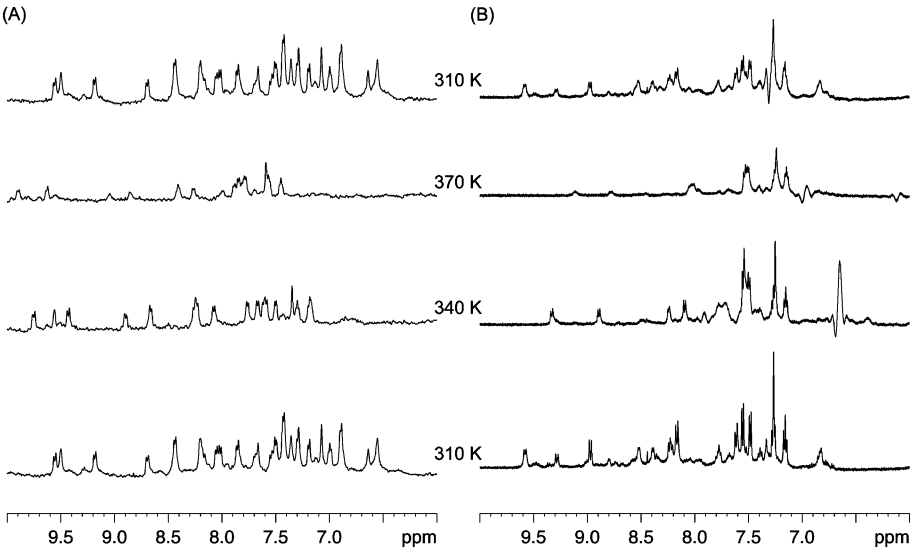

FIGURE 2: Attempted thermal denaturation of kB1 (A) and des(24−28)kB1 (B). 1D ^{1}H NMR spectra at 310, 340, and 370 K and again at 310 K after cooling. The complete reversibility of the thermal denaturation is shown with identical spectra after heating to temperatures approaching boiling (top trace).

reduced, alkylated kalata B1 (kB1-RA) were also incubated at 80 °C in 0.5 M HCl for comparison.

Mass Spectrometry. All solutions were monitored by LC−MS on an Agilent Series 1100 HPLC system coupled to an API QStar mass spectrometer (PE Sciex) equipped with an electrospray ionization (ESI) source. Data were collected, processed, and analyzed using the Analyst QS Software package (Applied Biosystems/MDS Sciex).

RESULTS

The thermal, chemical, and enzymatic stability of kB1 were investigated by NMR spectroscopy, fluorescence spectroscopy, and LC−MS. A number of derivatives of kB1, including the natural variant kalata B2 (kB2), two acyclic permutants, and a disulfide-deficient mutant, were also examined to quantify the contribution of various structural elements to stability. The acyclic permutant des(24−28)kB1 has five residues removed from the backbone in loop 6 (see Figure 1), a region corresponding to a processing site in the biosynthetic precursor protein (*22*). This permutant has previously been shown to adopt a fully folded yet not biologically active conformation, suggesting a role of the cyclic backbone in the mode of action (*43*). The second acyclic permutant, des(19−20)kB1, has two residues removed from loop 5 of the peptide backbone. It was examined because it contains an arginine residue necessary for tryptic cleavage that had been removed in the first acyclic permutant and provides an opportunity to examine the effect of breaking the backbone in a location different from that of the first acyclic permutant. The two-disulfide mutant has the two cysteines involved in the Cys^{I}−Cys^{IV} disulfide bridge in native kB1 replaced with alanines. The structure of this mutant has been determined (*40*), and it adopts a conformation similar to that of the native peptide; however, the effects of the missing disulfide bond on stability have not previously been investigated.

Thermal Stability. Figure 2 shows the 1D ^{1}H NMR spectra of kB1 and des(24−28)kB1 at selected temperatures in the range of 310−370 K and after cooling to 310 K. As expected, a number of the amide signals have temperature-dependent chemical shift changes. Surprisingly though, only relatively small changes to the peak widths were seen as the temperature was increased. The spectra recorded at high temperatures (>340 K) showed some line broadening, but nearly all signals could be detected even at temperatures approaching boiling. Once the compounds were cooled to 310 K, the 1D NMR spectrum was identical to the spectrum prior to heating, clearly showing the complete reversibility of any unfolding or conformational changes during heating. The solution was then subjected to mass spectrometric analysis to ensure that no modifications had occurred. The spectrum (not shown) was identical with that obtained prior to the heating.

The acyclic permutant des(24−28)kB1 was also subjected to attempts at thermal denaturation, as shown in Figure 2. A number of peaks diminished in intensity upon heating and were absent from the spectra recorded at >310 K. The remaining peaks were relatively unchanged in line width up to 330 K, above which their intensities decreased. Generally, a given degree of line broadening occurred at a temperature approximately 10 °C lower in des(24−28)kB1 then in kB1. However, the spectrum recorded after cooling to 310 K was identical to that prior to heating, illustrating the complete reversibility of the process, as was the case for the native kB1. The fact that the acyclic permutant had a thermal stability only slightly decreased relative to that of native kB1 suggests that the cystine knot rather than the cyclic backbone plays a major role in the thermal stability. To test whether this was specific to the cystine knot motif of the cyclotides, similar studies were carried out with another cystine knot peptide. Conotoxin PVIIA was utilized because its size (27 amino acids) and disulfide connectivity are similar to those of kB1 (*44*). In contrast to kB1 and its acyclic permutant, PVIIA underwent irreversible changes with temperature. Above temperatures of 330 K, the amide proton peaks broadened and substantially diminished in intensity (data not shown). When the compounds were cooled to 310 K, the peaks in the spectra remained broad and did not recover to their initial intensities or chemical shifts.

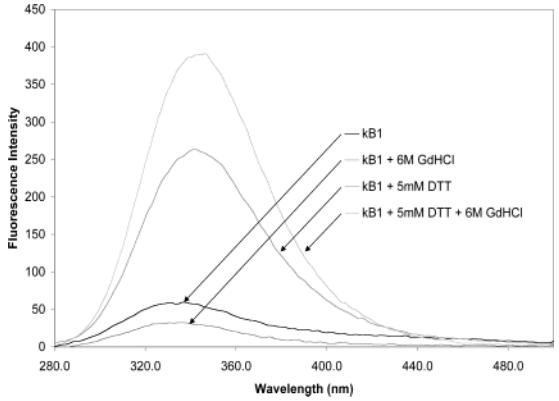

FIGURE 3: Effect of dithiothreitol (DTT) on the fluorescence of tryptophan. Fluorescence spectra of kB1 (25 μM) in the presence and absence of 5 mM DTT and/or 6 M GdHCl. The native peptide has a very low fluorescence intensity due to quenching of the Trp residue by the neighboring disulfide, an effect removed upon reduction by DTT.

Chemical Stability. Fluorescence spectroscopy was utilized to investigate the unfolding behavior of kB1 in the presence of chemical chaotropes and reductants. In particular, the solvent environment of the single tryptophan in this peptide was probed in the native and reduced forms and in the presence of denaturants. Figure 3 shows the results of the addition of 6 M GdHCl and/or 5 mM DTT to a 25 μM solution of kB1. The fluorescence spectrum of kB1 alone was low in intensity [compared, for example, to that of mellitin, a Trp-containing peptide that has been extensively studied by fluorescence (*45*), which exhibited a spectrum 4 times more intense], with a maximum emission wavelength (λ_{max}) of 335 nm. Upon addition of 6 M GdHCl, there was no significant change in either the fluorescence intensity or emission wavelength, although the former decreased slightly. The addition of DTT to kB1 followed by incubation at 37 °C for 30 min resulted in a large and significant increase in the fluorescence intensity (~5-fold), and the wavelength of maximum emission was red-shifted to ~345 nm. Addition of GdHCl to a solution of the DTT-reduced peptide caused a further increase in the intensity, but no change in the emission maximum. Kalata B2 behaved in a manner similar to that of kB1. Upon reduction, an increase in fluorescence intensity was observed, but the increase was ~2-fold compared to an increase of 5-fold for kB1. Unlike the case for kB1, the subsequent addition of GdHCl caused no further change in the fluorescence spectrum.

Figure 4 shows the fluorescence spectra of the acyclic permutant des(24−28)kB1 and the two-disulfide analogue in solutions of phosphate buffer, 6 M GdHCl, 5 mM DTT, or both the reducing agent and denaturant. The two species gave similar low-intensity spectra as seen for native kB1, with maximum fluorescence emission occurring at ~335 nm. Upon addition of DTT, large increases in fluorescence intensity were observed, ca. 5-fold for the acyclic permutant and ca. 6-fold for the two-disulfide permutant, and red shifts in the maximum fluorescence to 341 and 346 nm, respectively, were observed. This is consistent with the 5-fold intensity increase and 6 nm red shift observed for kB1 upon reduction.

Incubation of des(24−28)kB1 with GdHCl resulted in no significant changes to the fluorescence spectrum, as was also the case for native kB1, and the λ_{max} did not change

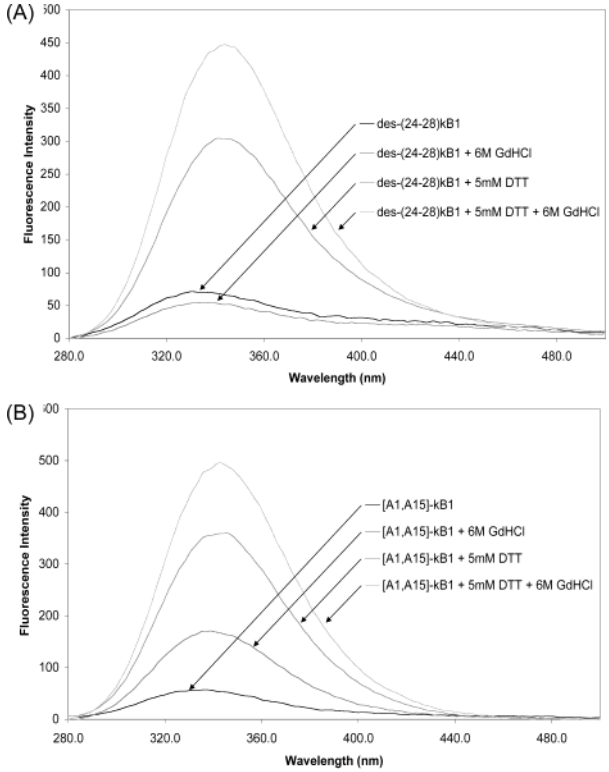

FIGURE 4: Fluorescence spectra of kB1 permutants (25 μM) in the presence and absence of 5 mM DTT and/or 6 M GdHCl: (A) the acyclic permutant des(24−28)kB1 and (B) the two-disulfide mutant [$A^{1,15}$]kB1. The removal of a single disulfide bond in [$A^{1,15}$]kB1 allows significant changes in the fluorescence spectra upon addition of GdHCl, an effect not observed for the native and acyclic peptides that were examined.

significantly. Incubation of the acyclic permutant with both GdHCl and DTT resulted in an intensity increased compared to that of the reduced species, without a discernible change in the wavelength of maximum fluorescence (344 nm). The two-disulfide mutant was the only species to show an increased fluorescence intensity upon addition of 6 M GdHCl to the oxidized form (3-fold increase). The wavelength of maximum emission was red-shifted (6 nm shift) compared to the spectrum in buffer alone. Addition of 6 M GdHCl to the reduced [$A^{1,15}$] mutant caused an increase in fluorescence intensity comparable to those observed for both reduced kB1 and reduced des(24−28)kB1.

Circular dichroism was utilized as an additional tool to examine the thermal and chemical denaturation of kB1. A 50 μM solution of kB1 in 10 mM potassium phosphate was examined by CD spectroscopy between 190 and 250 nm. The molar ellipticity at 220 nm was monitored with increasing temperature (5 °C increments up to 90 °C). No significant changes were observed in the CD spectra for either the pure kB1 solutions or solutions containing 8 M urea (see the Supporting Information). This supports the findings from the NMR and fluorescence data that the oxidized peptide is extremely resistant to conformational changes.

Enzymatic Stability. kB1 and the mutants were tested for their stability against four proteases: trypsin, endoGlu-C, pepsin, and thermolysin. The results were compared with those for two control peptides. A linear 34-amino acid peptide, corresponding to a truncated form of the bacterial chaperone *Escherichia coli* DnaK 577−610 (DnaK-f) (*46*), was utilized as a positive control peptide expected to be

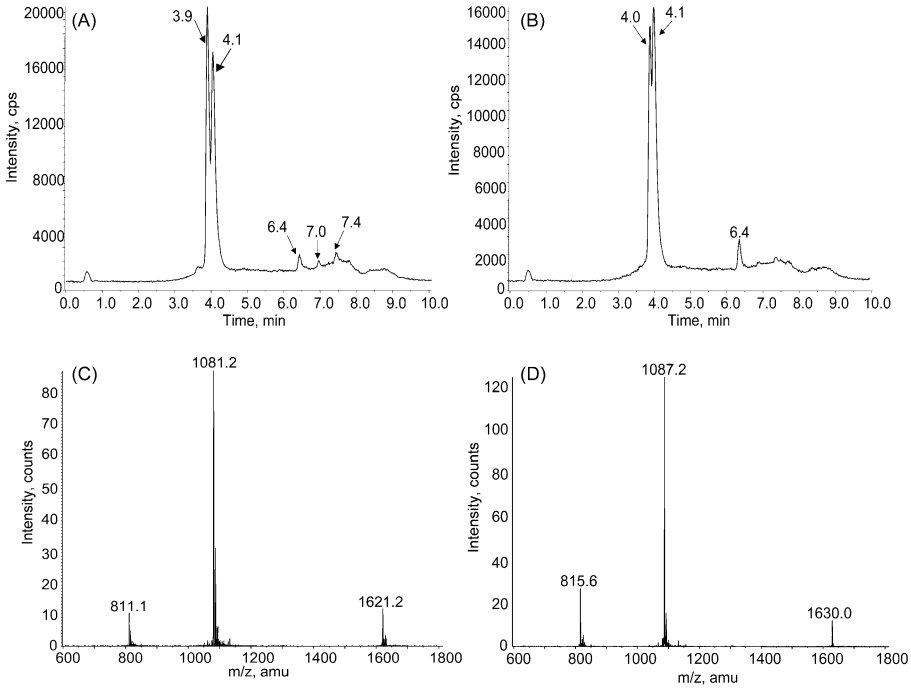

FIGURE 5: LC−MS chromatograms after incubation of kB1-RA with trypsin after 1 min (A) and endoGlu-C after 60 min (B) and the resulting mass spectra from the peak at 4.1 (C) and 3.9 min (D) from the tryptic digest. Native kB1 was not degraded in any case, while reduced kB1 exhibited an increased susceptibility toward proteolysis. The peaks observed at retention times of >6 min are due to digestion products of either the peptide or the enzyme itself.

susceptible to enzymatic degradation, and the conotoxin PVIIA was used as an example of a cystine knot-containing peptide. DnaK-f underwent cleavage in the presence of trypsin at one or more sites within 15 min, and complete proteolysis (i.e., at all sites) occurred in <1 h. This demonstrated the suitability of the enzyme digestion conditions. Under similar conditions, native kB1 did not undergo any cleavage, as monitored by LC−MS over the course of 6 h. The reaction mixture was again examined after 24 h, and after 48 h with the addition of fresh enzyme. No cleavage products were observed.

By contrast, the reduced and alkylated kalata B1 (kB1-RA) showed rapid degradation. Figure 5 shows the LC−MS chromatograms resulting after a 1 min incubation of kB1-RA with trypsin, and after a 60 min incubation with endoGlu-C. The peak at a retention time (t_R) of 4.1 min (Figure 5A) corresponded with a HPLC peak found in the absence of enzyme. The resulting mass spectrum (Figure 5C) showed two predominant peaks at *m*/*z* 1081.2 and 1621.2 corresponding to the triply and doubly charged ions, respectively, of reduced, alkylated kalata B1 (M_r = 3240 Da). Upon addition of trypsin, a second peak was observed at a t_R of 3.9 min, corresponding to a linearized version in which the peptide had been cleaved on the C-terminal side of the arginine residue. This second peak gave ions at *m*/*z* 1087.2 and 1630.0, which corresponds to the addition of H_2O across a peptide bond (M_r = 3258 Da). After a 15 min incubation at 37 °C, only a trace amount of cyclic peptide was still present. Des(24−28)kB1 was not used for tryptic digestion studies as it did not contain a proteolytic site because of the removal of the arginine. However, no tryptic digestion was observed for des(19−20)kB1, which does contain a potential trypsin cleavage site. Native PVIIA also showed no sign of degradation in the presence of trypsin, while reduced PVIIA was degraded in less than 1 min in the presence of trypsin or pepsin and in less than 15 min after incubation with thermolysin.

The degradation of kB1-RA by endoGlu-C was observed to proceed more slowly than that of trypsin. The LC−MS chromatogram (Figure 5B) shows a single peak at a t_R of 4.1 min in the absence of enzyme, while a second peak appeared at a t_R of 4.0 min upon addition of endoGlu-C. As was the case for tryptic digestion, a single product resulted from the cleavage of the cyclic backbone, but now the site of cleavage was on the C-terminal side of the glutamic acid residue. The endoGlu-C digestion gave mass spectra (not shown) nearly identical to that of the tryptic digest of the peptide as cleavage occurred at just one site in the backbone, resulting in linearization.

Figure 6 shows the time course for the enzymatic degradation of kB1, kB1-RA, and DnaK-f by endoGlu-C and of kB1, kB1-RA, DnaK-f, and PVIIA by thermolysin over a period of 5 h. The proportion degraded was calculated from the amount of cleavage products as detected by LC−MS. While the control peptide was completely degraded within minutes, the native kB1 remained unchanged for >5 h and the reduced peptide was degraded at an intermediate rate. Like native oxidized kB1, the two acyclic permutants (data not shown) showed no sign of degradation in the presence of trypsin, endoGlu-C, pepsin, or thermolysin, while the reduced form underwent rapid cleavage in the presence of trypsin (<15 min), endoGlu-C (<4 h), and thermolysin (<5 h), but was stable to pepsin. DnaK-f was degraded rapidly (<5 min) in both endoGlu-C and thermolysin, confirming that conditions were suitable for proteolytic degradation. As expected, the conotoxin PVIIA was not degraded in endoGlu-C under the conditions that were utilized. This peptide does not contain any glutamic acid residues and thus contains no potential sites for cleavage. However, the peptide was rapidly degraded (<30 min) in the presence of thermolysin.

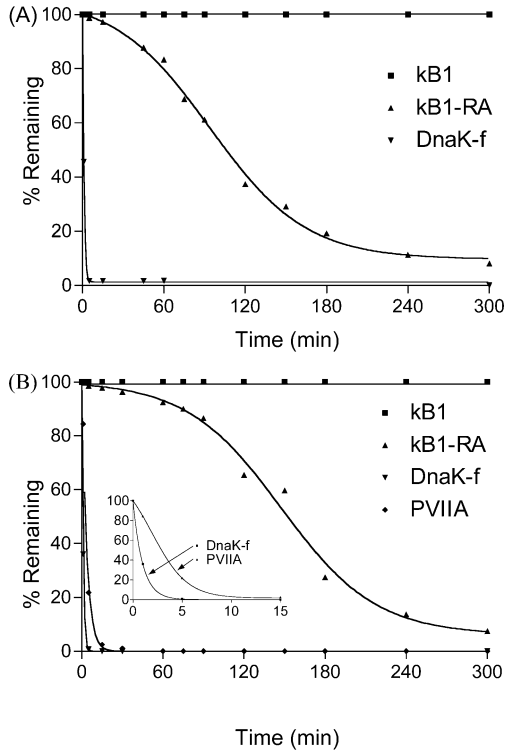

FIGURE 6: Enzymatic degradation of kB1, kB1-RA, DnaK-f, and PVIIA over time by (A) endoGlu-C and (B) thermolysin. The control peptide DnaK-f, and cystine knot peptide PVIIA, underwent rapid degradation in endopeptidases. kB1 was impervious to proteolytic cleavage, and kB1-RA exhibited resistance to proteolytic cleavage.

In the presence of pepsin, the digestive enzyme found in the gut, no degradation of native kB1 was observed. This was also the case for kB1-RA, which was stable for up to 24 h. There was no sign of degradation of the acyclic permutants in the presence of pepsin either. The control peptide, DnaK-f, was completely degraded within 15 min, with the cleavages occurring initially on the C-terminal side of glutamic acid and leucine residues. Conotoxin PVIIA was also incubated with pepsin and was found to undergo complete proteolysis within 5 min. Native oxidized kB1 and reduced kB1 were also incubated with pepsin in the presence of 3 M GdHCl, and both were found to be stable for up to 24 h.

Upon incubation of DnaK-f with thermolysin at 65 °C, multiple cleavages were observed on the N-terminal side of hydrophobic residues, in particular at leucine and isoleucine residues. By contrast, kB1 was completely impervious to proteolysis by thermolysin, as were the acyclic permutants. It is interesting to note that in the case of kB1-RA, very little degradation was observed over the first 90 min, after which proteolysis followed a sigmoidal pattern (Figure 6). There are five theoretical cleavage sites (C_5-V_6, $S_{18}-W_{19}$, $P_{20}-V_{21}$, $G_{26}-L_{27}$, and $P_{28}-V_{29}$) within the peptide sequence, and polypeptide fragments from cleavage at four of these sites were observed in the mass spectra (the exception being the $S_{18}-W_{19}$ site).

Acid Hydrolysis. The peptides were dissolved in 0.5 M hydrochloric acid and incubated at 80 °C to examine their hydrolysis over time. No hydrolysis, as monitored by LC−MS, was observed for samples that had been incubated for up to 0.5 h; only a single peak corresponding to native kB1 was observed. Two new peaks were observed in the HPLC trace for a sample taken after a 45 min incubation, and these increased in intensity with an increased incubation time. They yielded identical mass spectra corresponding to a single cleavage of the cyclic peptide backbone (mass increase of 18); however, their different retention times suggested that two species were present, the later eluting peak being approximately 3-fold more abundant. After 1 h, an additional peak was noted with a mass consistent with two cleavages of the backbone (i.e., the addition of 36 to the molecular mass). This peak increased in intensity with time, and after 2 h, a second earlier eluting peak was observed in the chromatogram. This had the same mass, indicating that two species containing two cleavages of the peptide backbone were present. All of the samples taken after 2 h contained another peak in the chromatogram, because of a further cleavage, i.e., three cleavages of the backbone.

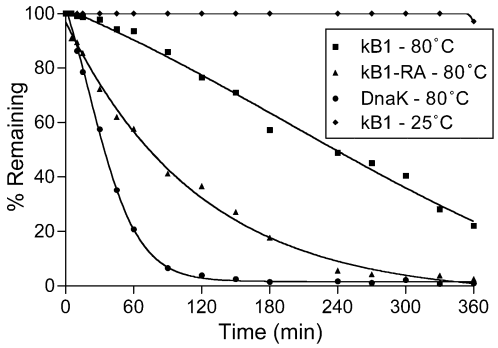

FIGURE 7: Acid hydrolysis of kB1 at 25 (◆) and 80 °C (■) and hydrolysis of the control peptide DnaK-f (●) and kB1-RA (▲). Reduced kB1 exhibited greater resistance to acid hydrolysis than DnaK-f did, while native kB1 again was highly stable.

Figure 7 shows the acid-induced degradation of kB1, kB1-RA, and DnaK-f as seen in LC−MS chromatograms over time. For the control DnaK-f peptide, cleavage of the backbone to yield multiple different peptide species was observed. More than 95% of the control peptide was degraded after 2 h compared to ~25% degradation of kB1. Approximately 65% of kB1-RA had been hydrolyzed after the same time, and complete hydrolysis occurred in <6 h. All of the reduced and oxidized kalata peptides were also examined after incubation in acid at 25 °C, but degradation did not occur at this temperature. Under more acidic conditions (1 and 2 M HCl), the rate of hydrolysis of kB1 was increased and the point at which 95% of the peptide had been hydrolyzed was observed to be at 5 and 2 h, respectively (data not shown).

In summary, the thermal, chemical, and enzymatic stabilities of the prototypic cyclotide kalata B1 have been quantitatively determined, and the results provide definitive evidence of its exceptional stability. Comparisons of the native form to fully reduced or two-disulfide species have highlighted the reduced stability of derivatives lacking one or more disulfide bridges.

DISCUSSION

In this work, we have examined the thermal, chemical, and enzymatic stabilities of the prototypic cyclotide kB1. It was compared to several related peptides, including the natural variant kB2 that contains five substituted residues, two acyclic permutants, in which the backbone is broken in

two different places, and a mutant in which a single disulfide bond has been removed. The native, folded form of the peptide was stable in aqueous solution to temperatures approaching boiling, to high concentrations of the chaotropic agents guanidine hydrochloride (6 M) and urea (8 M), and to enzymatic degradation, as well as showing resistance to hydrolysis in 0.5 M HCl. By contrast, the reduced species showed decreased stability and was susceptible to enzymatic degradation by trypsin, endoGlu-C, and thermolysin as well as showing increased susceptibility toward acid hydrolysis. Two acyclic permutants displayed proteolytic stability comparable with that of kB1, suggesting that the cystine knot rather than the cyclic backbone is largely responsible for the resistance to endopeptidases. These quantitative findings on the stability of the cyclotide kB1 and the relative contributions of its constituent structural motifs, namely, a circular backbone and a cystine knot, provide information that will be useful in the exploitation of the CCK framework as a molecular template.

The resistance of kB1 to thermal denaturation as monitored by NMR spectroscopy shows that the cyclotides are thermally stable to at least 370 K. The acyclic permutant des(24−28)kB1 was slightly more sensitive to temperature changes, but its NMR spectra also showed complete reversibility after it cooled to 310 K. The additional flexibility conferred by the break in the backbone could account for the increased susceptibility of the acyclic permutant to temperature. Overall, the cystine knot in kB1 shows remarkable thermal stability. By contrast, PVIIA appeared to be irreversibly denatured after being heated to 370 K, despite having a cystine knot motif similar to that of kB1. This demonstrates that some cystine knots are not as stable as others, and that other structural features must also contribute to the particular stability of the cyclotides. One such factor could be a strong hydrogen bond network that has been identified between the carboxyl side chain of Glu^3 and the backbone amide protons of Thr^{11} and Asn^{12} (*47*). Glu^3 is one of few residues completely conserved among all known cyclotides and appears to play a crucial role, via its hydrogen bonding interactions, in defining and stabilizing their three-dimensional structures.

The thermal stability studies were followed by attempts to chemically denature kB1 and its variants. Given the chemical similarity between denaturants such as urea or GdHCl and peptide bonds, which are mostly buried in folded proteins, their denaturing action can be described using the adage "like dissolves like", if unfolding is viewed as the dissolving of peptide bonds into the solvent. Since individual interactions between these denaturants and proteins are weak, the total strength of the interaction is greater if the number of interactions can be increased, as occurs with protein unfolding. In the current study, fluorescence methods were used to monitor the unfolding process.

Fluorescence spectroscopy provides a convenient and sensitive means for probing the environment of Trp residues in proteins (*48*). Since kB1 contains no Tyr or Phe residues, its fluorescence is determined by the environment of its single Trp. The fluorescence intensity of kB1 and its variants was low compared to that of mellitin, which was used as a positive control. For proteins in general, the Trp λ_{max} is sensitive to the local environment, ranging from 308 nm for azurin (Trp completely buried) to 353 nm for glucagon (fully solvent-exposed) (*49*), and moves toward longer wavelengths when the Trp is exposed to a polar medium. In the current study, mellitin was found to have a λ_{max} of 350 nm, in agreement with the literature (*50*). kB1 and kB2 had emission maxima of ~335 nm, indicating that the Trp in these molecules is in a partially solvated environment. This is consistent with structural studies, which indicate that in the folded state the three-disulfide bonds occupy the protein core, thus forcing the Trp and other hydrophobic residues to the surface. Although the Trp residue is exposed (see Figure 1), it is protected on one face by the adjacent Pro residue, thus explaining the "partially exposed" position of the fluorescence maximum. NMR spectra provide evidence of this Trp−Pro interaction via the significant upfield shift of one of the Pro β-protons, seen at approximately −0.25 ppm (a shift of >2 ppm from the random coil value) (*6*). Also of relevance to the interpretation of the current fluorescence data is the fact that the Trp residue is in the proximity of the Cys5−Cys17 disulfide bond. Disulfides are known to be effective quenchers of Trp fluorescence (*51*). The combination of this quenching and the exposed location of the Trp residue accounts for the low observed fluorescence intensity in the native state of kB1 and its derivatives studied here.

In most folded proteins, addition of denaturants generally results in a decrease in fluorescence intensity and in a red shift of the fluorescence maximum. There was no significant change in the fluorescence spectra of any of the oxidized derivatives (kB1, kB2, or the acyclic permutants) on addition of GdHCl, suggesting that either they are not denatured by this agent or there is simply insufficient change in the already low fluorescence signal, which has the characteristics of an exposed Trp, even in the native state. On the basis of other observations reported herein, the former explanation seems more likely; i.e., the cyclic cystine knot has very little capacity to denature, even under the most extreme chaotropic conditions. The small drop in fluorescence intensity seen upon addition of GdHCl may reflect some slight local disordering of the Trp side chain, disrupting its interactions with the adjacent Pro residue.

The large increase in fluorescence intensity observed for kB1 upon addition of DTT, i.e., on formation of the reduced form of the peptide, is due to the disruption of the disulfide bonds, which removes the source of the quenching of the Trp residue. The reduced peptide yields fluorescence spectra with a λ_{max} shifted to the red compared to that of the native peptide, indicating an increased level of solvent exposure. The addition of GdHCl to the reduced form of kB1 brought about an increase in the fluorescence intensity, which increased linearly with increasing GdHCl concentration. kB2 behaved like kB1, indicating that the five residue substitutions did not appear to dramatically influence the fluorescence behavior of the molecule. The increased fluorescence intensity upon addition of a denaturant to reduced kB1 is unusual, but there are other known examples in which an increase in fluorescence intensity is observed upon denaturation. For example, Lakshmikanth and Krishnamoorthy examined the dynamics of solvent-exposed Trp residues at protein surfaces and observed an increase in fluorescence emission upon addition of denaturant (*52*). Another example is the DsbA protein form *E. coli* in which reduction of the active site disulfide in the thioredoxin domain causes a more

than 3-fold increase in tryptophan fluorescence (*53*). In this example, the Trp that is quenched is more than 12 Å from the active site disulfide; however, energy transfer occurs through a phenylalanine residue.

The acyclic permutant, des(24−28)kB1, was studied to determine the contribution of the cyclic backbone to the chemical stability of kB1. The addition of denaturant to this permutant resulted in little change in the fluorescence spectra, indicating little change in the chemical environment of the Trp residue. Upon reduction, a large increase in fluorescence intensity and a red shift in the λ_{max} were evidence of a change in the environment from a partially solvated state to a fully solvent-exposed state and removal of the quenching effect of the disulfide bond. The addition of GdHCl to the reduced form of des(24−28)kB1 brought about a similar increase in fluorescence intensity like that observed for reduced kB1. These results are in agreement with structural studies on the acyclic derivative, which showed that breaking the backbone in loop 6 of the cyclotide structure has a minimal effect on the three-dimensional fold (*41*).

Studies on the two-disulfide mutant clearly showed the contribution of the disulfide bonds to the chemical stability of kB1. This derivative has the same fold as native kB1, with only minor changes noted near Cys1/Ala1 (*40*), showing that the missing disulfide bond is not essential for maintaining the three-dimensional fold. However, by contrast with all of the other oxidized three-disulfide peptides that were studied, the addition of denaturant to this two-disulfide mutant caused an increase in fluorescence intensity. Thus, despite not greatly affecting the structure, the removal of the Cys^{I}−Cys^{IV} disulfide bond appears to predispose the molecule to a degree of conformational unfolding that becomes apparent upon addition of a denaturant. The increase in intensity and red-shifted maximum suggest that the conformational change affects both the local Trp environment and the degree of quenching caused by the remaining two disulfide bonds. Complete reduction resulted in a fluorescence spectrum similar to that of reduced kB1, as might be expected because all disulfide cross-links are absent in both species.

Figure 8 summarizes the effects of the addition of reductant and denaturant to native kB1, des(24−28)kB1, and $[A^{1,15}]$kB1. It indicates that denaturant alone has essentially no effect on the three-disulfide species, but can cause minor disruption of the two-disulfide species. The position of a hydrogen bond network from Glu^{3} that may be a key factor in stabilizing the cystine knot of cyclotides relative to other cystine knot-containing peptides is indicated. Reduction of all disulfide bonds causes substantial increases in fluorescence intensity, mainly due to removal of disulfide bond quenching of Trp. However, there must be a degree of conformational ordering in the reduced species, as addition of denaturing agents to them causes a further change in fluorescence signals.

Although the results reported here show that it is the cystine knot rather than the circular backbone that plays a major role in structural stabilization of the cyclotides, the circular backbone also plays a role. It is interesting to compare the results with recent reports on a peptide that has a circular backbone but no cystine knot. AS-48 is a 70-amino acid circular enterocin produced by *Enterococcus faecalis* that contains no cysteines or post-translationally modified

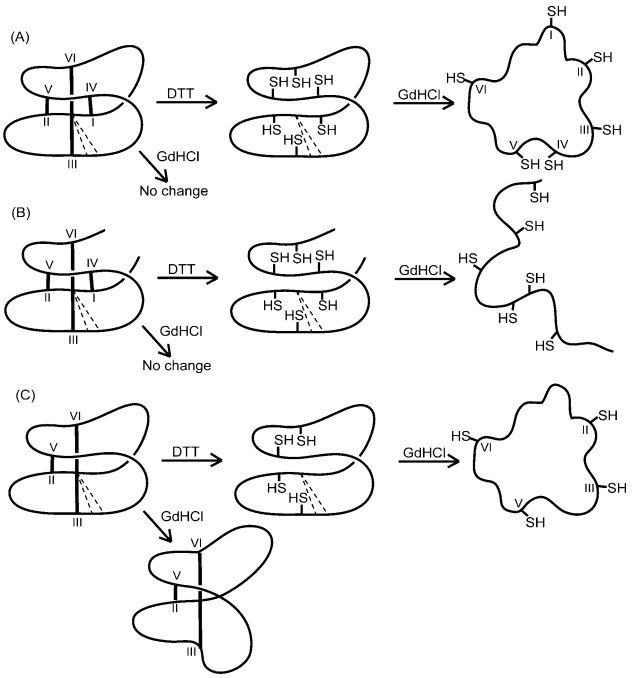

FIGURE 8: Schematic representation of the effects of a denaturant (GdHCl) and a reducing agent (DTT) on kB1 (A), des(24−28)-kB1 (B), and $[A^{1,15}]$kB1 (C). These represent a native cyclotide, an acyclic permutant, and a two-disulfide mutant, respectively. The solid lines represent intact disulfide bonds, while dashed lines show the hydrogen bond network among Glu^{3}, Asn^{11}, and Thr^{12}. Both three-disulfide species are essentially unaffected by GdHCl, but the two-disulfide mutant is susceptible to partial denaturation. The fact that the acyclic permutant and native cyclotide behave similarly suggests that most of the resistance to chemical denturation comes from the cystine knot rather than the circular backbone. Reduction of all of the species with DTT causes large changes in the fluorescence spectra, but the reduced species may adopt a partially native fold, judging by the fact that subsequent addition of denaturant to the reduced peptides causes further changes in the fluorescence spectra.

amino acids. The peptide is extremely stable against heat- and denaturant-induced unfolding and only unfolded at 102 °C, pH 2.5, and a low ionic strength. At 25 °C, it unfolded in 6 M GdHCl but did not unfold in 8 M urea (*42*). By contrast, kB1 was stable under the same conditions (8 M urea and pH 2.5) up to 98 °C and did not unfold in GdHCl. The knotted arrangement of disulfide bonds present in the cyclotides thus clearly confers additional stability against thermal and chemical denaturation.

Surprisingly, there have been few reports about the enzymatic stability of cystine knot proteins. A synthetic form of ω-conotoxin MVIIA was found to degrade in endoproteinase Lys-C and in trypsin, in both the oxidized and reduced forms (*54*). TxVII, another ω-conotoxin, was also found to undergo proteolysis only after long incubation times with endoproteinase Lys-C followed by thermolysin (*55*). For comparison, insulin-like growth factor (IGF-I) is a large polypeptide also containing three disulfide bridges; however, these are arranged in a Cys^{I}−Cys^{IV}, Cys^{II}−Cys^{VI}, and Cys^{III}−Cys^{V} connectivity, and thus, IGF-I does not fall within the cystine knot classification. It has been shown to be degraded in cocktails containing pancreatic enzymes, intestinal flushings, and/or endoproteases such as trypsin and chymotrypsin (*56*). Many cystine knot peptides, or knottins, are found in protease-rich environments, and this structural motif may well have evolved to confer protease resistance (*57*). In

general, cystine knot-containing proteins appear to be considerably more stable than other peptides similar in size and disulfide content.

Native kB1 was observed to be impervious to degradation by trypsin, endoGlu-C, pepsin, and thermolysin. The experiments utilizing pepsin in the presence of acid were designed to represent conditions present in the stomach. kB1 was also incubated in the presence of intestinal contents for up to 24 h and was completely stable. In all experiments, a linear control peptide similar in size (DnaK-f) underwent rapid degradation. The two acyclic permutants tested also exhibited exceptional stability, with no signs of any degradation occurring as monitored by LC−MS. kB1-RA was susceptible to tryptic cleavage as well as to digestion by two of the three other proteases that were used. This degradation was monitored over 6 h, and nearly all peptide was cleaved after a 15 min incubation with trypsin, a 4 h incubation with endoGlu-C, and a 5 h incubation with thermolysin. The reduced peptide was resistant to pepsin both in aqueous buffer and in the presence of a denaturant (3 M GdHCl). The cystine knot conotoxin PVIIA was also impervious to the enzymes tested here in its native form. However, upon removal of the disulfide linkages, it was degraded extremely rapidly in both trypsin and pepsin (<1 min) and by thermolysin (<15 min).

The stability of kB1 toward strongly acidic conditions was also examined. A solution of kB1 in 0.5 M HCl was incubated at both 25 and 80 °C and analyzed by LC−MS following neutralization. This concentration of acid corresponds to a pH of ∼0.3 and is approximately twice the concentration of acid present in the stomach. Under these conditions, most peptides would be expected to cleave into multiple products ranging from dipeptide and tripeptide fragments up to larger oligopeptides (*58*). However, the only products resulting from the incubation in acid were species containing up to four cleavages of the cyclic backbone. Analysis of the fragments suggested that the backbone segments were held together by disulfide bonds. This again highlights the importance of the disulfide bridges in stabilizing the cyclotides. The control peptide DnaK-f, a linear disulfide-free peptide, was degraded almost completely within 2 h under similar conditions, at which point only 25% of the kB1 had been hydrolyzed. kB1-RA exhibited increased susceptibility toward hydrolysis, with 65% degraded after 2 h, and complete degradation was seen in <6 h. This increased rate of hydrolysis, compared to that of native kB1, highlights the role of the disulfide core in maintaining the structure and integrity of these molecules.

In conclusion, the prototypic cyclotide kalata B1 is thermally, chemically, and enzymatically stable. By contrast, the reduced species is more susceptible to chemical agents and enzymatic degradation. The removal of a single disulfide has a destabilizing effect, even though it does not greatly affect the three-dimensional structure. The quantitative determination of the stability of kalata B1 reported here provides a foundation for potential applications of the cyclotide framework in molecular design applications where a stable protein-based scaffold is required.

ACKNOWLEDGMENT

We thank Norelle Daly [Institute for Molecular Bioscience (IMB)] for supplying the acyclic permutants and two-disulfide mutant and for helpful discussions and preliminary data on unfolding studies on kalata B1. We are also grateful for the assistance of Alun Jones (IMB) with the mass spectrometric analysis.

SUPPORTING INFORMATION AVAILABLE

CD spectra of kalata B1, in the absence and presence of 8 M urea, between 190 and 250 nm at 25 °C are shown. Below 210 nm, interference was caused by the presence of the urea. There were no significant differences noted in the spectra at any measured temperature (5−95 °C). This material is available free of charge via the Internet at http://pubs.acs.org.

REFERENCES

1. Craik, D. J., Daly, N. L., Bond, T., and Waine, C. (1999) *J. Mol. Biol. 294*, 1327−1336.
2. Gran, L. (1970) *Medd. Nor. Farm. Selsk. 12*, 173−180.
3. Gran, L. (1973) *Acta Pharmacol. Toxicol. 33*, 400−408.
4. Gran, L. (1973) *Lloydia 36*, 174−178.
5. Sletten, K., and Gran, L. (1973) *Medd. Nor. Farm. Selsk. 7*−*8*, 69−82.
6. Saether, O., Craik, D. J., Campbell, I. D., Sletten, K., Juul, J., and Norman, D. G. (1995) *Biochemistry 34*, 4147−4158.
7. Craik, D. J., Daly, N. L., and Waine, C. (2001) *Toxicon 39*, 43−60.
8. Gran, L. (1973) *Lloydia 36*, 207−208.
9. Gustafson, K. R., Sowder, R. C., II, Henderson, L. E., Parsons, I. C., Kashman, Y., Cardellina, J. H., II, McMahon, J. B., Buckheit, R. W., Jr., Pannell, L. K., and Boyd, M. R. (1994) *J. Am. Chem. Soc. 116*, 9337−9338.
10. Witherup, K. M., Bogusky, M. J., Anderson, P. S., Ramjit, H., Ransom, R. W., Wood, T., and Sardana, M. (1994) *J. Nat. Prod. 57*, 1619−1625.
11. Claeson, P., Göransson, U., Johansson, S., Luijendijk, T., and Bohlin, L. (1998) *J. Nat. Prod. 61*, 77−81.
12. Daly, N. L., Koltay, A., Gustafson, K. R., Boyd, M. R., Casas-Finet, J. R., and Craik, D. J. (1999) *J. Mol. Biol. 285*, 333−345.
13. Göransson, U., Luijendijk, T., Johansson, S., Bohlin, L., and Claeson, P. (1999) *J. Nat. Prod. 62*, 283−286.
14. Tam, J. P., Lu, Y. A., Yang, J. L., and Chiu, K. W. (1999) *Proc. Natl. Acad. Sci. U.S.A. 96*, 8913−8918.
15. Hallock, Y. F., Sowder, R. C. I., Pannell, L. K., Hughes, C. B., Johnson, D. G., Gulakowski, R., Cardellina, J. H. I., and Boyd, M. R. (2000) *J. Org. Chem. 65*, 124−128.
16. Gustafson, K. R., Walton, L. K., Sowder, R. C. I., Johnson, D. G., Pannell, L. K., Cardellina, J. H. I., and Boyd, M. R. (2000) *J. Nat. Prod. 63*, 176−178.
17. Hernandez, J. F., Gagnon, J., Chiche, L., Nguyen, T. M., Andrieu, J. P., Heitz, A., Trinh Hong, T., Pham, T. T., and Le Nguyen, D. (2000) *Biochemistry 39*, 5722−5730.
18. Broussalis, A. M., Goransson, U., Coussio, J. D., Ferraro, G., Martino, V., and Claeson, P. (2001) *Phytochemistry 58*, 47−51.
19. Bokesch, H. R., Pannell, L. K., Cochran, P. K., Sowder, R. C., II, McKee, T. C., and Boyd, M. R. (2001) *J. Nat. Prod. 64*, 249−250.
20. Craik, D. J. (2001) *Toxicon 39*, 1809−1813.
21. Felizmenio-Quimio, M. E., Daly, N. L., and Craik, D. J. (2001) *J. Biol. Chem. 276*, 22875−22882.
22. Jennings, C., West, J., Waine, C., Craik, D., and Anderson, M. (2001) *Proc. Natl. Acad. Sci. U.S.A. 98*, 10614−10619.
23. Craik, D. J., Anderson, M. A., Barry, D. G., Clark, R. J., Daly, N. L., Jennings, C. V., and Mulvenna, J. (2002) *Lett. Pept. Sci. 8*, 119−128.
24. Lindholm, P., Goransson, U., Johansson, S., Claeson, P., Gulbo, J., Larsson, R., Bohlin, L., and Backlund, A. (2002) *Mol. Cancer Ther. 1*, 365−369.
25. Schöpke, T., Hasan Agha, M. I., Kraft, R., Otto, A., and Hiller, K. (1993) *Sci. Pharm. 61*, 145−153.
26. Trabi, M., and Craik, D. J. (2002) *Trends Biochem. Sci. 27*, 132−138.
27. McDonald, N. Q., and Hendrickson, W. A. (1993) *Cell 73*, 421−424.

28. Murray-Rust, J., McDonald, N. Q., Blundell, T. L., Hosang, M., Oefner, C., Winkler, F., and Bradshaw, R. A. (1993) *Structure 1*, 153−159.
29. Le Nguyen, D., Heitz, A., Chiche, L., Castro, B., Boigegrain, R. A., Favel, A., and Coletti-Previero, M. A. (1990) *Biochimie 72*, 431−435.
30. Pallaghy, P. K., Nielsen, K. J., Craik, D. J., and Norton, R. S. (1994) *Protein Sci. 3*, 1833−1839.
31. Isaacs, N. W. (1995) *Curr. Opin. Struct. Biol. 5*, 391−395.
32. van den Hooven, H. W., van den Burg, H. A., Vossen, P., Boeren, S., de Wit, P. J. G. M., and Vervoort, J. (2001) *Biochemistry 40*, 3458−3466.
33. Kooman-Gersmann, M., Vogelsang, R., Hoogendijk, E. C. M., and De Wit, P. J. G. M. (1997) *Mol. Plant-Microbe Interact. 10*, 821−829.
34. Adams, D. J., Alewood, P. F., Craik, D., Drinkwater, R. D., and Lewis, R. J. (1999) *Drug Dev. Res. 46*, 219−234.
35. Price-Carter, M., Salem Hull, M., and Goldenberg, D. P. (1998) *Biochemistry 37*, 9851−9861.
36. Muller, Y. A., Heiring, C., Misselwitz, R., Welfle, K., and Welfle, H. (2002) *J. Biol. Chem. 277*, 43410−43416.
37. Heiring, C., and Muller, Y. A. (2001) *Protein Eng. 14*, 183−188.
38. Craik, D. J., Simonsen, S., and Daly, N. L. (2002) *Curr. Opin. Drug Discovery Dev. 5*, 251−260.
39. Nourse, A., Trabi, M., Daly, N. L., and Craik, D. J. (2004) *J. Biol. Chem. 279*, 562−570.
40. Daly, N. L., Clark, R. J., and Craik, D. J. (2003) *J. Biol. Chem. 278*, 6314−6322.
41. Daly, N. L., and Craik, D. J. (2000) *J. Biol. Chem. 275*, 19068−19075.
42. Cobos, E. S., Filimonov, V. V., Galvez, A., Maqueda, M., Valdivia, E., Martinez, J. C., and Mateo, P. L. (2001) *FEBS Lett. 505*, 379−382.
43. Barry, D. G., Daly, N. L., Clark, R. J., Sando, L., and Craik, D. J. (2003) *Biochemistry 42*, 6688−6695.
44. Scanlon, M. J., Naranjo, D., Thomas, L., Alewood, P. F., Lewis, R. J., and Craik, D. J. (1997) *Structure 5*, 1585−1597.
45. Dempsey, C. E. (1990) *Biochim. Biophys. Acta 1031*, 143−161.
46. Kragol, G., Lovas, S., Varadi, G., Condie, B. A., Hoffmann, R., and Otvos, L. (2001) *Biochemistry 40*, 3016−3026.
47. Rosengren, K. J., Daly, N. L., Plan, M. R., Waine, C., and Craik, D. J. (2003) *J. Biol. Chem. 278*, 8606−8616.
48. Lakowicz, J. R. (2000) *Photochem. Photobiol. 72*, 421−437.
49. Vivian, J. T., and Callis, P. R. (2001) *Biophys. J. 80*, 2093−2109.
50. Etfink, M. R. (1991) *Methods Biochem. Anal. 35*, 127−205.
51. Cowgill, R. W. (1967) *Biochim. Biophys. Acta 140*, 37−44.
52. Lakshmikanth, G. S., and Krishnamoorthy, G. (1999) *Biophys. J. 77*, 1100−1106.
53. Hennecke, J., Sillen, A., Huber-Wunderlich, M., Engelborghs, Y., and Glockshuber, R. (1997) *Biochemistry 36*, 6391−6400.
54. Zheng, K., Lubman, D. M., Rossi, D. T., Nordblom, G. D., and Barksdale, C. M. (2000) *Rapid Commun. Mass Spectrom. 14*, 261−269.
55. Sasaki, T., Feng, Z.-P., Scott, R., Grigoriev, N., Syed, N. I., Fainzilber, M., and Sato, K. (1999) *Biochemistry 38*, 12876−12884.
56. Anderle, P., Langguth, P., Rubas, W., and Merkle, H. P. (2002) *J. Pharm. Sci. 91*, 290−300.
57. Chiche, L. (2003) http://knottin.cbs.cnrs.fr/.
58. Derua, R., Gustafson, K. R., and Pannell, L. K. (1996) *Biochem. Biophys. Res. Commun. 228*, 632−638.

BI049711Q